Predicting Filtration Time and Maximizing Throughput in a Pressure Filter

Kerry A. Landman and Lee R. White
Advanced Mineral Products Centre, Dept. of Mathematics, University of Melbourne, Parkville 3052, Victoria, Australia

The modeling of pressure filtration of flocculated suspensions using compressional rheology and a knowledge of compressional yield stress $P_y(\phi)$ and a hydraulic resistance factor $r(\phi)$ (ϕ is the local volume fraction of solids) is shown to yield an initial solids loading that maximizes the throughput of the filter. The optimal initial height h_0 is such that the filtration time to reach a specified average volume fraction as output equals the handling time for the filter press. The maximum throughput of the press is then examined as a function of the remaining control parameters, the initial solids volume fraction ϕ_0, and the applied piston pressure ΔP. The dependence of filtration time on ϕ_0/ϕ_∞ (where ϕ_∞ is the volume fraction of solids at infinite time under applied pressure ΔP) enables the construction of a simple numerical model for the pressure filtration process, which accurately approximates predictions of the full compressional rheology model.

Introduction

Solid/liquid separation by pressure filtration is a common industrial process that many workers (e.g., Terzaghi and Peck, 1948; Sivaram and Swamee, 1977; Phillip and Smiles, 1982; Smiles and Kirby, 1987; Banks, 1985; Shirato et al., 1982; Landman et al., 1991, 1995) have modeled.

The key to a physical understanding of the pressure filtration process is the recognition of a solids or particle stress in addition to the hydrostatic or fluid stress. These two stresses add to comprise the applied piston pressure and their contributions to the total pressure vary through the filter cell and as a function of time of filtration. Although it was common in the modeling to assume the particle stress was a function of local particle concentration, the physical nature of that assumption was not clear until Buscall and White (1987) explained the particle stress as a compressive yield stress $P_y(\phi)$.

They postulated that the network of particles by virtue of the interparticle attractive forces in the case of flocculated systems (or frictional and steric forces in the case of stable irregularly shaped particles) could behave as a solid at a volume fraction ϕ until the applied particle stress exceeded the compressive yield stress for that volume fraction, at which stage collapse of the structure and local volume fraction increase will occur. The further assumption that the collapse process is rapid compared to typical process times implies that the particle stress at a point in the suspension is always only infinitesimally above the compressive yield stress at the local volume fraction. The functional form of $P_y(\phi)$ is shown in Figure 1. This stress is a good representation of the particle mechanics for fractal networks, where spontaneous rearrangement of the network is occurring on long time scales with respect to the process time. For stable dispersions, $P_y(\phi)$ is the osmotic pressure.

Buscall and White (1987) identified the other significant rheological property in solid/liquid separation, the hydraulic resistance or hindered settling factor $r(\phi)$. The hydrodynamic force F_{Hy} on the particle network per unit suspension volume is given by

$$F_{Hy} = -[\lambda(v - w)]r(\phi)\frac{\phi}{V_p}, \tag{1}$$

where
λ = Stokes drag parameter for average particle
$v(w)$ = average local particle (fluid) velocity
V_p = average particle volume

We require

$$r(\phi) \underset{\phi \to 0}{\to} 1$$

Correspondence concerning this article should be addressed to L. R. White.

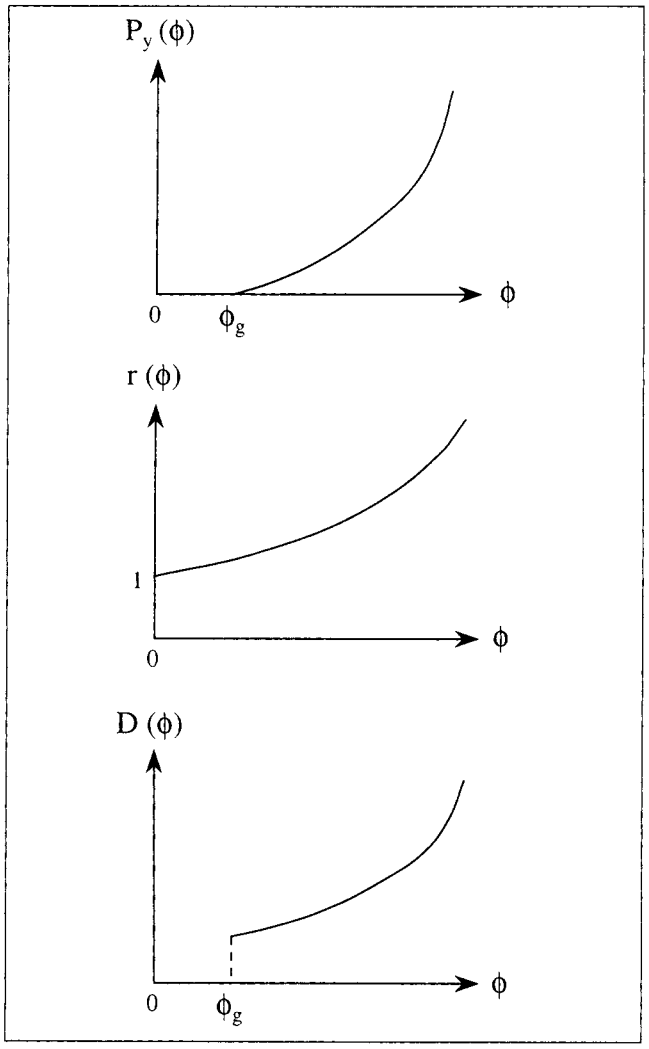

Figure 1. Rheological parameters in solid/liquid separation shown as a function of volume fraction.

and expect it to be a monotonic increasing function of local volume fraction (the functionality being dependent on the particle network structure) reflecting the hydrodynamic interference on any given particle by its neighbors (see Figure 1). Alternatively, it may be treated as an inverse Darcy permeability for flow through the local particle network.

Methods for measuring $P_y(\phi)$ and $r(\phi)$ are discussed in Landman and White (1994). These methods have been used successfully by a number of experimenters. The resulting yield stress estimates have been fitted with power-law and exponential functions (Eberl et al., 1995; Eckert et al., 1996; Miller et al., 1996; Channell and Zukoski, 1997; Green, 1997). The hindered settling factor has also been fitted with various empirical relationships (Auzerais et al., 1990; Eberl et al., 1995; Green, 1997); the models are fairly insensitive to the form of $r(\phi)$. Later we choose some typical type of functional forms for these rheological functions.

If we consider a one-dimensional treatment of the pressure filtration process, we must describe $\phi(z,t)$ the volume fraction at height z above the filter membrane as a function of time (see Figure 2). In this article we consider the filtration process starting at zero time, with a constant piston pressure

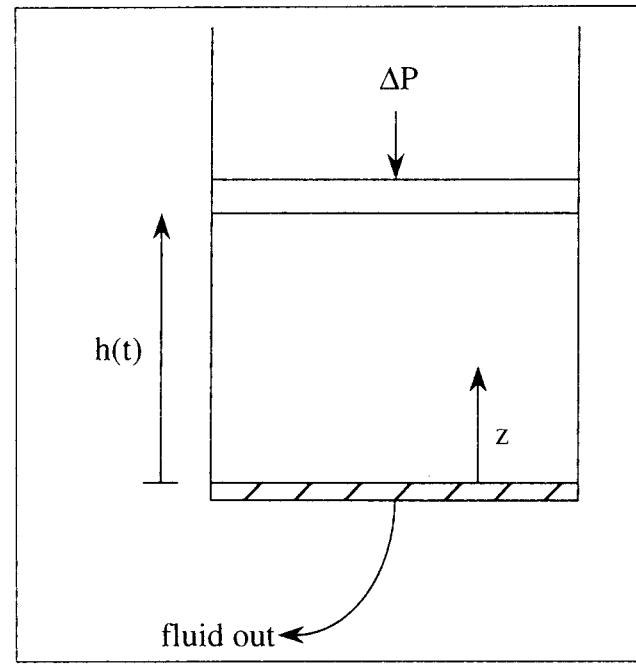

Figure 2. Geometry of the filter-press model.

ΔP applied to the suspension in which the initial volume fraction ϕ_0 is uniform with an initial piston height h_0. From a process point of view, we monitor $h(t)$ and seek to determine how the control factors ϕ_0, h_0, ΔP may affect the throughput of the pressure filtration process.

The fluid flux through the filter membrane is dh/dt at time t and the corresponding fluid pressure drop across the membrane is $-Rdh/dt$, where R is the hydraulic resistance of the membrane. At the membrane, the sum of particle and fluid stresses is then

$$P_y[\phi(0,t)] - R\frac{dh}{dt} = \Delta P. \tag{2}$$

If we can neglect the membrane resistance in comparison with the resistance of the filter bed, then the volume fraction of solids at the membrane is determined by

$$P_y[\phi(0,t)] = \Delta P(t). \tag{3}$$

In the present case, where ΔP is a constant from $t = 0$, the volume fraction at the membrane is ϕ_∞ (the infinite time volume fraction in the filter bed) given by

$$P_y(\phi_\infty) = \Delta P. \tag{4}$$

From the form of $P_y(\phi)$ given in Figure 1, we must consider two regimes of compression. If ϕ_0 is smaller than ϕ_g (the volume fraction below which particle concentration is too small to permit a percolated network to span the filter press), then particles (flocs) cannot transmit stress. Thus, in this ϕ_0 regime, there will be a region near the piston where the entire applied stress is carried by the fluid pressure. In the absence of gravity (which may be neglected where sedimentation times are large compared to filtration times), there is no

physical mechanism to change the local concentration of particles in this unnetworked region.

Of course the fluid flux through the membrane leads to the buildup of particle concentration there and the establishment of the particle network. The volume fraction at the membrane moves (essentially instantly) to its final value of ϕ_∞ as the piston pressure ΔP is applied. With time a bed of networked particles grows from the membrane toward the piston. Thus for $\phi_0 < \phi_g$, the initial stage of filtration is characterized by the growth of the compact bed, above which there is a region extending to the piston, with the initial volume fraction of particles ϕ_0. Note that the volume fraction of particles in the compact bed is not uniform, varying from ϕ_∞ to ϕ_g at the top of the bed, since the particle stress falls to zero at this point.

At a certain time t_c the compact bed height reaches the piston. For $t > t_c$, the piston pressure is shared by the fluid and particles at all points in the filter press, and the network spanning the vessel is compressed. The compression stage lasts from t_c to infinite time, at which stage, the piston ceases to move and uniform volume fraction ϕ_∞ is established everywhere in the press. The network pressure at infinite time is everywhere ΔP and the fluid pressure is everywhere zero.

In the second filtration regime $\phi_0 > \phi_g$, and the network spans the press from $t = 0$. Application of a piston pressure results in compression everywhere in the press, as local volume fractions increase monotonically with time to the infinite time value of ϕ_∞ as before. No shock wave corresponding to the top of a compact bed moves through the press in this filtration regime.

The equations governing the filtration process have been derived by many workers (e.g., Landman et al., 1995) and may be summarized by a diffusion equation for the local volume fraction

$$\frac{\partial \phi}{\partial t} = \frac{\partial}{\partial z}\left[D(\phi)\frac{\partial \phi}{\partial z} - \phi\frac{dh}{dt}\right], \tag{5}$$

where

$$D(\phi) = \left(\frac{V_p}{\lambda}\right)\left[\frac{dP_y(\phi)/d\phi}{r(\phi)}\right](1-\phi)^2 \tag{6}$$

plays the role of a ϕ-dependent diffusion coefficient whose form is shown in Figure 1. The initial and boundary conditions on Eq. 5 are

$$\phi(0,t) = \phi_\infty \qquad (t > 0) \tag{7}$$

$$\frac{\partial \phi}{\partial z}(h,t) = 0 \qquad (t > 0) \tag{8}$$

$$\int_0^{h(t)} dz\,\phi(z,t) = \phi_0 h_0 \qquad (t > 0) \tag{9}$$

$$\phi(z,0) = \phi_0 \qquad (0 < z < h_0) \tag{10}$$

As discussed in Landman et al. (1995), boundary condition (Eq. 8) is a consequence of fluid and particle velocities at the piston being equal to the flux per unit area through the membrane. Condition 9 serves to determine $h(t)$ and reflects conservation of total particle volume during the process.

It will prove convenient to introduce the following scalings

$$Z = \frac{z}{h_0} \tag{11}$$

$$H(T) = \frac{h(t)}{h_0} \tag{12}$$

$$T = \frac{tD_\infty}{h_0^2}\left(\frac{\phi_\infty}{\phi_0}\right)^2, \tag{13}$$

where

$$D_\infty = D(\phi_\infty). \tag{14}$$

The filtration model is then written as

$$\frac{\partial \phi}{\partial T} = \frac{\partial}{\partial Z}\left(d(\phi)\frac{\partial \phi}{\partial Z} - \phi\frac{dH}{dT}\right), \tag{15}$$

where

$$d(\phi) = \frac{D(\phi)}{D_\infty}\left(\frac{\phi_0}{\phi_\infty}\right)^2, \tag{16}$$

with

$$\phi(0,T) = \phi_\infty \tag{17}$$

$$\frac{\partial \phi}{\partial Z}(H,T) = 0 \tag{18}$$

$$\frac{1}{\phi_0}\int_0^{H(T)} dZ\,\phi(Z,T) = 1 \tag{19}$$

$$\phi(Z,0) = \phi_0 \qquad (0 < Z < 1). \tag{20}$$

These equations form a complete solution of pressure filtration, but the numerical solution of the nonlinear diffusion equation with up to two moving boundaries is complicated and does not lend itself easily to engineering design.

In the rest of this article two important aspects of pressure filtration are investigated—optimizing the filtration throughput and a simple approximate method for determining the filtration time. We examine these quantities as functions of the control parameters h_0, ϕ_0, ϕ_∞. This knowledge allows for some powerful conclusions about the design of pressure-filter operations.

Optimization of Filtration Throughput

The throughput Q of a batch device such as a filter press can be defined as the total amount of solid processed in the operation divided by the total time it takes to perform the process. For a filter press, this total time is made up of two components, the time to filter from initial volume fraction to the output volume fraction of solids t_f, and the handling time for the operation t_h, which comprises all the assembly, load-

ing, unloading, and disassembly operations that must occur to process a batch. To a reasonable approximation we can take t_h to be independent of the amount of material to be processed.

Thus we can write for the throughput per unit area of filter membrane

$$Q = \frac{\phi_0 h_0}{t_f + t_h}, \tag{21}$$

where $\phi_0 h_0$ is the solids volume processed in one batch. Application of a piston pressure ΔP would achieve a uniform final volume fraction ϕ_∞ given by Eq. 4, but only at infinite time. In practice the filtration would be stopped at a finite time t_f (T_f in scaled time), when the average volume fraction in the press is given by

$$\langle \phi \rangle = f\phi_\infty, \tag{22}$$

where f is a fraction close to unity. In terms of the scaled piston height,

$$H(T_f) = \frac{1}{f} H_\infty, \tag{23}$$

where

$$H_\infty = \frac{\phi_0}{\phi_\infty} \tag{24}$$

is the scaled piston height at infinite time. The filtration model described by the scaled equations (Eqs. 15–20) does not involve the initial height h_0 of the system, so that the scaled filtration time T_f is given by

$$T_f = T_f(\phi_0, \phi_\infty, f), \tag{25}$$

the functionality depending on the form of $d(\phi)$. It follows from Eq. 13 that in real time

$$t_f = h_0^2 \tau_f, \tag{26}$$

where

$$\tau_f = \left(\frac{\phi_0}{\phi_\infty}\right)^2 \frac{T_f}{D_\infty}. \tag{27}$$

The throughput is then a peaked function of the initial load height h_0:

$$Q = \frac{\phi_0 h_0}{h_0^2 \tau_f + t_h} \tag{28}$$

and is maximal ($dQ/dh = 0$) when

$$t_f = t_h \tag{29}$$

or

$$h_0^{\max} = \left(\frac{t_h}{\tau_f}\right)^{1/2}. \tag{30}$$

The optimal throughput is then

$$Q_{\max} = \frac{\phi_0}{2(\tau_f t_h)^{1/2}}, \tag{31}$$

and we can write

$$Q(h_0) = Q_{\max} \frac{2(h_0/h_0^{\max})}{1 + (h_0/h_0^{\max})^2}, \tag{32}$$

which is displayed in Figure 3.

If one is interested in operating a filter press at maximum throughput, then the simple result follows from our model—load the filter so that the filtration time is equal to the handling time. This result provides a simple rule of thumb for pressure-filter operation. As far as we know, this is a new finding and is not known or used in the industry.

A similar result obtains for the vacuum filter where initial height h_0 is not an appropriate parameter. In this form of filtration, where solids are deposited on the filter membrane from an essentially infinite amount of suspension at volume fraction ϕ_0 by the fluid flow through the membrane, the amount processed is determined by the filtration time t_f—the time for which unit area of filter membrane is subjected to the vacuum.

In vacuum filtration we are always operating in the compact-bed formation regime. It is well known (e.g., Landman et al., 1995) that in this regime, the volume of filtrate expressed is proportional to the square root of filtration time, provided the membrane resistance is negligible. The material deposited on the membrane in time t_f is proportional to the filtrate volume and therefore increases as $t_f^{1/2}$. We assume here that no shearing processes in the slurry affect the buildup

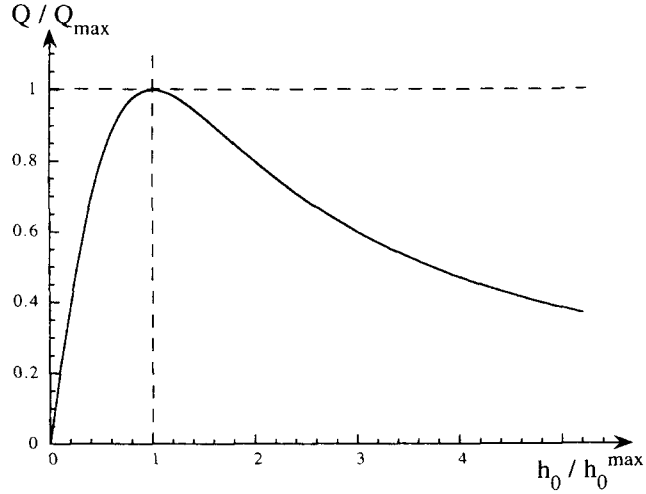

Figure 3. Filter-press throughput Q as a function of initial loading height h_0.

of the compact bed. After application of the vacuum, the material is removed and the membrane cleaned before reapplying the suction. We denote this time as the handling time t_h for the process and again assume it is essentially independent of the amount of solids deposited.

Thus, for vacuum filtration, we can write for the throughput

$$Q^{\text{vac}}(t_f) = \frac{Kt_f^{1/2}}{t_f + t_h}, \tag{33}$$

where K is a function of ϕ_0 and the vacuum pressure but is independent of t_f. The throughput is maximal ($dQ^{\text{vac}}/dt_f = 0$) when Eq. 29 is satisfied and

$$Q_{\max}^{\text{vac}} = \frac{K}{2t_h^{1/2}}. \tag{34}$$

In the remainder of this article we concentrate on the pressure filtration case only.

Dependence of $Q_{\max}$ on ϕ_0, ΔP

The filtration model has allowed us to dispose of the parameter h_0. We can now examine filtration performance as a function of ϕ_0 and ΔP by examining $Q_{\max}$. Combining Eqs. 31 and 27, we can write

$$Q_{\max} = \frac{\phi_\infty D_\infty^{1/2}}{2t_h^{1/2} T_f^{1/2}}, \tag{35}$$

where we have the scaled filtration time T_f as a function of ϕ_0 and ϕ_∞, as well as the stopping fraction f, as in Eq. 25.

To illustrate the dependence of T_f and $Q_{\max}$ on ϕ_0 and ϕ_∞ we resort to numerical calculation on a model system. We choose typical parameter values

$$P_y(\phi) = k\left[\left(\frac{\phi}{\phi_g}\right)^5 - 1\right] \tag{36}$$

$$r(\phi) = (1-\phi)^{-3.5}, \tag{37}$$

where

$$\phi_g = 0.1, \tag{38}$$

and we choose piston pressures

$$\frac{\Delta P}{k} = 10, 100. \tag{39}$$

It is not necessary to specify the constant k or the value of (λ/V_p), which enters the definition of D_∞, since the scaled diffusion equation that models the process does not require them.

Using Eq. 4, the final volume fraction ϕ_∞ corresponding to the choices of ΔP previously, is, from Eq. 36,

$$\phi_\infty^{10} = 0.1615 \tag{40}$$

$$\phi_\infty^{100} = 0.2517. \tag{41}$$

The stopping fraction f used in these calculations was

$$f = 0.95, 0.99. \tag{42}$$

The numerical technique for solving Eqs. 15–20 was described previously (Landman et al., 1991).

In Figure 4 we plot the filtration time t_f as a function of initial volume fraction ϕ_0 for stopping fractions $f = 0.95, 0.99$ for the two values of applied pressure. For the region $\phi_0 < \phi_g$, the filtration time is comprised of a compact-bed formation time t_c and a compression time. The magnitude of the compact-bed formation time is shown also. For $\phi_0 > \phi_g$ the compact-bed formation time t_c is zero and t_f is entirely compression time. Interestingly, as ϕ_0 tends to zero, the stopping

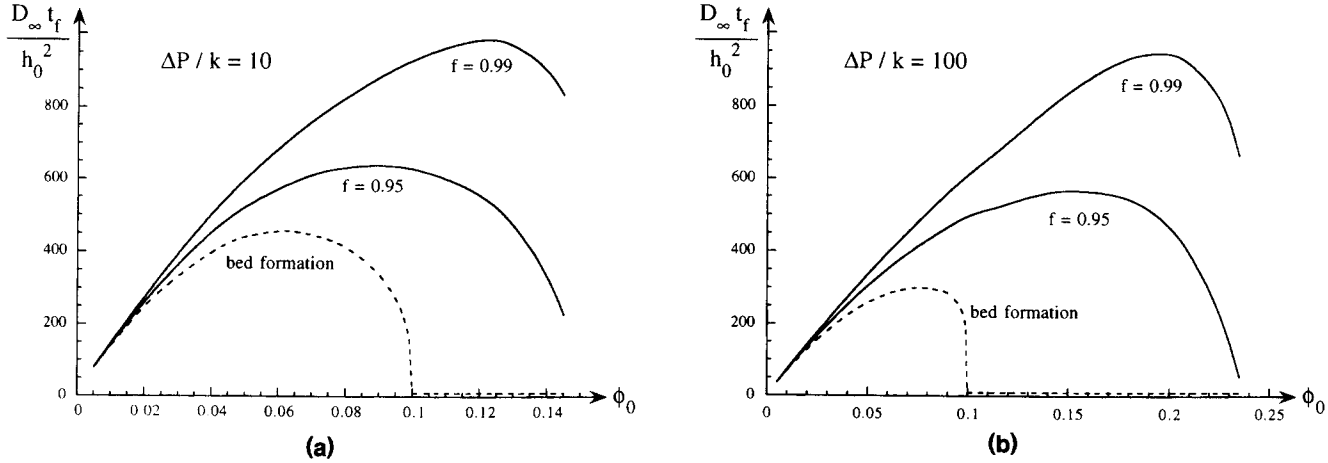

Figure 4. Scaled filtration time $D_\infty t_f/h_0^2$ as a function of initial volume fraction for two values of the stopping fraction f at applied piston pressure (a) $\Delta P/k = 10$ and (b) $\Delta P/k = 100$.

Shown dotted is the scaled compact-bed-formation time $D_\infty t_c/h_0^2$.

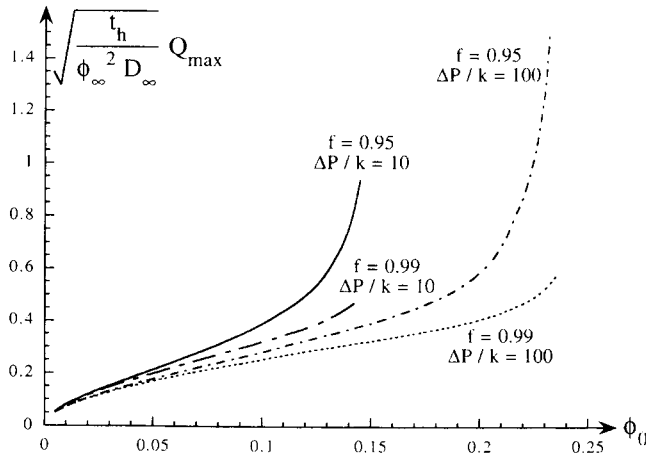

Figure 5. $[t_h/(\phi_\infty^2 D_\infty)]^{\frac{1}{2}} Q_{max}$ as a function of ϕ_0 for two values of the stopping fraction f at applied piston pressure $\Delta P/k = 10$ and $\Delta P/k = 100$.

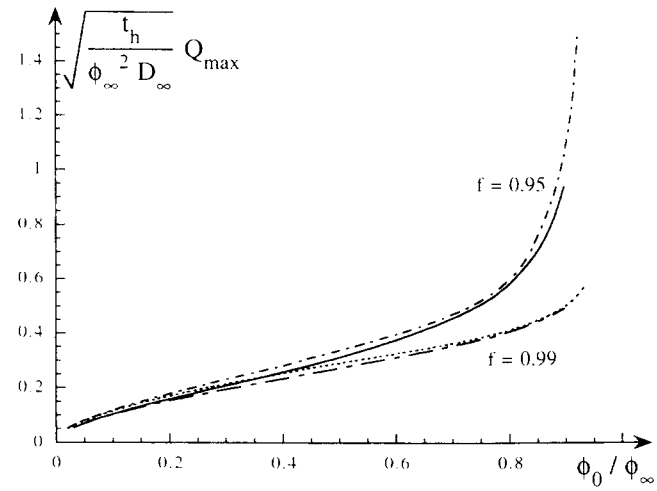

Figure 6. Scaled maximum throughput $[t_h/\phi_\infty^2 D_\infty)]^{1/2}$ Q_{max} as a function of ϕ_0/ϕ_∞.

fraction appears to be unimportant and compression time tends to zero. Filtration time is dominated by compact-bed formation in this limit and tends to zero, since the bed height (the source of hydraulic resistance) vanishes, and, in the absence of membrane resistance, filtration is essentially instantaneous. As $\phi_0 \to f\phi_\infty$, the filtration time must again tend to zero, since no filtration need occur to produce the output (Eq. 22) in this trivial limit.

From Eq. 35 we have that

$$\left(\frac{t_h}{\phi_\infty^2 D_\infty}\right)^{1/2} Q_{max} = \frac{1}{2T_f^{1/2}}. \tag{43}$$

In Figure 5 we plot this scaled maximum throughput as a function of initial volume fraction ϕ_0 for $f = 0.95$, 0.99 and the two values of applied pressure. We note that Q_{max} vanishes in the limit $\phi_0 \to 0$ since, although the filtration time is decreasing, the amount of material treated is vanishing with ϕ_0 at a faster rate. Throughput is obviously reduced by making the stopping fraction f approach unity, since the filtration time t_f is becoming infinite in this limit. As $\phi_0 \to f\phi_\infty$, throughput diverges, since filtration time is vanishing in this limit.

There is no qualitative difference in the filtration behavior for the two values of the applied pressure. Quantitatively the higher applied pressure produces lower filtration times and higher maximum throughput, but the ΔP dependence is not strong, the tenfold pressure increase leading to roughly doubling of the throughput. This is due to the higher volume fraction ϕ_∞ at the bottom of the bed in the high-pressure case and the increased hydraulic resistance resulting from this, which tends to offset the increased driving pressure.

These figures highlight the following commonsense finding, although again this does not appear to be emphasized in the industry. From a plant-operational point of view, maximum filter-press efficiency is achieved by increasing the initial volume fraction of solids. The "plateau" region around $\phi_0 = \phi_g$ in Figure 5, suggests that input to a filter could usefully be the output of a prior gravity-thickening process, in which volume fraction of solids would be just a little larger than ϕ_g and which would not sediment appreciably while stored awaiting filtration, if the solids height is not too large.

In Figure 6, we plot the scaled filtration throughput (Eq. 43) as a function of ϕ_0/ϕ_∞. The curves for a given stopping fraction f for the different piston pressures ΔP are almost coincident. This implies that

$$T_f \approx T_f\left(\frac{\phi_0}{\phi_\infty}, f\right). \tag{44}$$

Now the scaled equations (Eqs. 15–20) would permit a functionality of the form

$$T_f = T_f\left(\phi_\infty, \frac{\phi_0}{\phi_\infty}, f\right), \tag{45}$$

but do not strictly allow the functionality implied by Eq. 44 by virtue of their highly nonlinear nature. The empirical fact that T_f sensibly obeys Eq. 44 leads one to suspect that the full nonlinear diffusion problem might be replaced by a simpler linear problem that could provide an accurate engineering design solution. We pursue this end in the remainder of the article.

Reformulation of the Problem

The moving boundary in the filtration problem corresponding to the piston at $Z = H(T)$ may be removed and the differential equation simplified by changing to a material coordinate w (Kirby and Smiles, 1988) defined by

$$w(Z,T) = \frac{1}{\phi_0}\int_0^Z dZ\phi(Z,T). \tag{46}$$

We note that

$$w(0,T) = 0 \tag{47}$$

$$w(H(T),T) = 1 \tag{48}$$

by virtue of Eq. 19. If we make the change of variable

$$\phi(Z,T) \rightarrow \phi(w,T),$$

the problem may be stated as

$$\frac{\partial \phi}{\partial T} = \phi^2 \frac{\partial}{\partial w}\left(\frac{d(\phi)}{\phi_0^2}\frac{\partial \phi}{\partial w}\right) \tag{49}$$

$$\phi(0,T) = \phi_\infty \tag{50}$$

$$\frac{\partial \phi}{\partial w}(1,T) = 0 \tag{51}$$

$$\phi(w,0) = \phi_0. \tag{52}$$

A second simplification comes from the introduction of the void ratio e defined by

$$e = \frac{1-\phi}{\phi} = \frac{1}{\phi} - 1. \tag{53}$$

We note from Eq. 46 that

$$Z(w,T) = \phi_0 \int_0^w \frac{dw}{\phi(w,T)}, \tag{54}$$

and hence that

$$H(T) = \phi_0\left[1 + \int_0^1 e(w,T)dw\right]. \tag{55}$$

In terms of the void ratio the problem is stated as (Kirby and Smiles, 1988)

$$\frac{\partial e}{\partial T} = \frac{\partial}{\partial w}\left[\Delta(e)\frac{\partial e}{\partial w}\right] \tag{56}$$

$$e(0,T) = e_\infty = \frac{1}{\phi_\infty} - 1 \tag{57}$$

$$\frac{\partial e}{\partial w}(1,T) = 0 \tag{58}$$

$$e(w,0) = e_0 = \frac{1}{\phi_0} - 1, \tag{59}$$

where

$$\Delta(e) = \frac{\phi^2 D(\phi)}{\phi_\infty^2 D_\infty}. \tag{60}$$

Note that

$$\Delta(e_\infty) = 1. \tag{61}$$

These changes of variable have not removed the internal moving boundary that is present when $\phi_0 < \phi_g$ $(e_0 > e_g)$, which represents the top of the compact bed at $w = w_c(T)$.

Fortunately, a similarity solution for $e(w,T)$ exists for $T \le T_c$. In fact,

$$e(w,T) = \begin{cases} E\left(\dfrac{w}{w_c(T)}\right) & (w \le w_c) \\ e_0 & (w > w_c) \end{cases}, \tag{62}$$

where

$$w_c(T) = \left(\frac{T}{T_c}\right)^{1/2} \tag{63}$$

and $E(X)$ satisfies

$$\frac{d}{dX}\left[\Delta(E)\frac{dE}{dX}\right] + \frac{1}{2T_c}X\frac{dE}{dX} = 0 \tag{64}$$

$$E(0) = e_\infty \tag{65}$$

$$E(1) = e_g \tag{66}$$

$$\Delta(e_g)\frac{dE}{dX}(1) = \frac{e_0 - e_g}{2T_c}. \tag{67}$$

Equation 67 is the shock-curve equation and may be directly derived by integrating Eq. 56 across the discontinuity at $w = w_c$. Solving Eqs. 64–67 determines T_c and $e(w,T)$ for $T \le T_c$. In the domain $T > T_c$ we must solve Eqs. 56–58, with Eq. 59 replaced by the initial condition

$$e(w,T_c) = E(w), \tag{68}$$

since

$$w_c(T_c) = 1. \tag{69}$$

Thus, we must solve a nonlinear diffusion equation for $e(w,T)$. In general $\Delta(e)$, displayed in Figure 7, is a highly nonlinear function of its argument.

A simpler problem would be to replace $\Delta(e)$ by a constant to produce a linear diffusion equation that is easily solvable. The rapidly varying nature of $\Delta(e)$ makes the choice of this constant nonobvious. Further, we note that for large times, the diffusion equation tends to

$$\frac{\partial e}{\partial T} = \frac{\partial^2 e}{\partial w^2} \tag{70}$$

using Eq. 61. If the filtration time is large ($f \sim 1$), it will be important to reproduce this asymptotic time dependence.

It seems attractive to replace $\Delta(e)$ by unity (its value for $e = e_\infty$) for $e_\infty < e < e_0$. Numerical comparison of this approximation with the full nonlinear solution is shown in Figures 8a, 8b for the numerical example introduced earlier. The agreement is not good. The details of this approximation are not given here in view of the inaccuracy of the approximation.

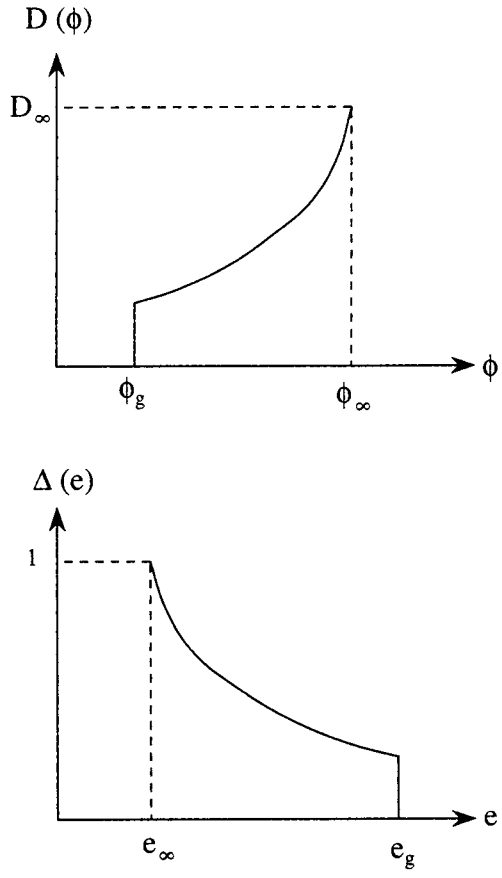

Figure 7. Functions $D(\phi)$ and $\Delta(e)$ that play the role of the diffusion coefficient; note that $\Delta(e)$ is zero for $e > e_g$ because the diffusion coefficient $D(\phi)$ vanishes for $\phi < \phi_g$ by virtue of its definition.

Mean Action Time $T^*(w)$

The mean action time in a diffusion equation (McNabb, 1975) is a measure of the time taken for the disturbance introduced at the boundary to diffuse past the observation point. As such it must be a function of position in space. The solution $e(w,T)$ as a function of T for a fixed volume of w is displayed in Figure 9. Clearly the mean action time $T^*(w)$ is located in the neighborhood of the peak in $\partial e(w,T)/\partial T$.

A suitable definition for our nonlinear problem is

$$T^*(w) = \frac{\int_0^\infty dT \cdot T \frac{\partial}{\partial T} \int_{e_\infty}^{e(w,T)} de\Delta(e)}{\int_0^\infty dT \frac{\partial}{\partial T} \int_{e_\infty}^{e(w,T)} de\Delta(e)}, \tag{71}$$

where the time-derivative term in the integrand plays the role of the peaked function that serves to concentrate T in the neighborhood of the peak in $\partial e(w,T)/\partial T$. An integration by parts gives us a more useful, but not too obvious, definition of the mean action time, namely,

$$T^*(w) = \frac{\int_0^\infty dT \int_{e_\infty}^{e(w,T)} de\Delta(e)}{\int_{e_\infty}^{e_0} de\Delta(e)}. \tag{72}$$

We see in Appendix A that $T^*(w)$ satisfies

$$\frac{d^2T^*}{dw^2} = -\frac{(e_0 - e_\infty)}{\int_{e_\infty}^{e_0} de\Delta(e)}, \tag{73}$$

with initial conditions

$$T^*(0) = 0 \tag{74}$$

$$\frac{dT^*}{dw}(0) = \frac{e_0 - e_\infty}{\int_{e_\infty}^{e_0} de\Delta(e)}. \tag{75}$$

This set of equations serves to uniquely determine $T^*(w)$ for a given $\Delta(e)$.

Let us suppose that the filtration time T_f for our nonlinear

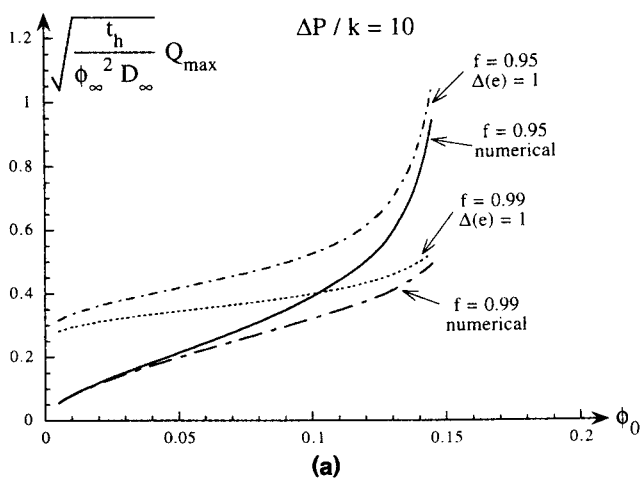

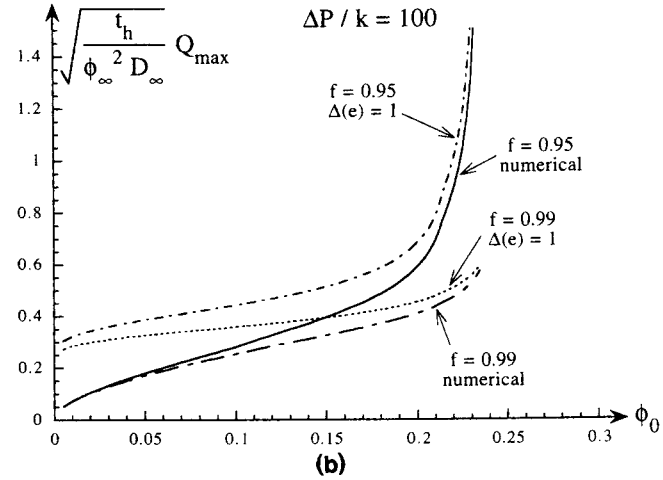

Figure 8. Comparison of the full numerical solution with the approximate linear solution using $\Delta(e)=1$ ($e_\infty < e < e_0$): (a) $\Delta P/k = 10$; (b) $\Delta P/k = 100$.

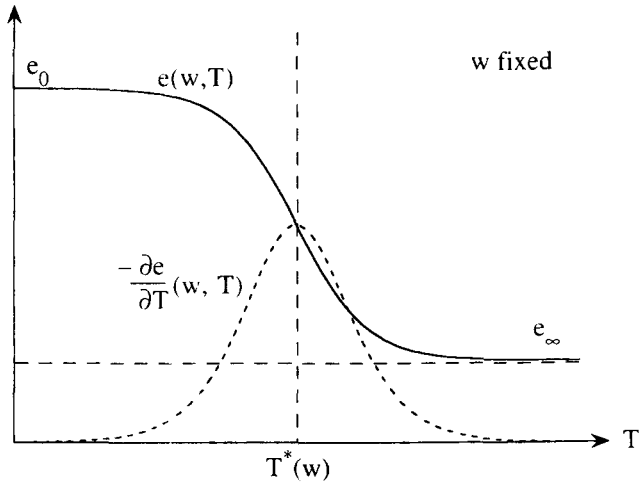

Figure 9. Solution $e(w, T)$ as a function of time at a fixed value of w showing the location of the middle of the diffusional front at the " mean action time" $T^*(w)$.

system lies in the neighborhood of $T^*(w)$. If we replace our nonlinear system by another system [i.e., another $\Delta(e)$], we could ensure that the two systems had identical mean action time by requiring that, in the replacement, the quantity

$$\int_{e_\infty}^{e_0} de\Delta(e)$$

was preserved. Given this constraint on the replacement system, it is reasonable to expect that the two systems would have very similar filtration times T_f if they have identical mean action times $T^*(w)$ for all points $0 < w < 1$.

Linear Approximations

If we are to replace our nonlinear problem by another, it would be because we can solve analytically the alternate problem. Solvability requires linearity in the diffusion equation case, so we are led to seek linear replacements for $\Delta(e)$. Three approximations that ensure mean action time equality suggest themselves.

Choice 1. We replace $\Delta(e)$ by

$$\Delta_{\text{eff}}^{(1)} = \int_{e_\infty}^{e_0} de\Delta(e)/(e_0 - e_\infty) \quad (e_\infty < e < e_0), \tag{76}$$

ensuring that the alternative problem with the constant diffusion coefficient will have the same mean action time as the nonlinear problem. The difficulty with this choice is that it ignores a major feature of $\Delta(e)$, namely, that it is zero for $e > e_g$.

Choice 2. We replace $\Delta(e)$ by

$$\Delta_{\text{eff}}^{(2)} = \theta(e_g - e)\int_{e_\infty}^{e_0} de\Delta(e)/\begin{pmatrix} e_0 - e_\infty & (e_0 < e_g) \\ e_g - e_\infty & (e_0 > e_g) \end{pmatrix}, \tag{77}$$

where $\theta(e)$ is the unit step function

$$\theta(e) = \begin{cases} 1 & (e > 0) \\ 0 & (e < 0) \end{cases}. \tag{78}$$

This choice of linear replacement is solvable, but lacks the feature that the problem reduces asymptotically to Eq. 70. Note that for $e_0 < e_g$ ($\phi_0 > \phi_g$), Choices 1 and 2 are identical.

Choice 3.

$$\Delta_{\text{eff}}^{(3)} = \theta(e^* - e), \tag{79}$$

where to ensure the mean action time quality we require

$$e^* = e_\infty + \int_{e_\infty}^{e_0} de\Delta(e). \tag{80}$$

This choice preserves the property $\Delta(e) = 0$ for $e > e_g$, but also reduces to Eq. 70 asymptotically. Note that the quantity e^* is always less than e_0.

In Figure 10, the three "linear" alternative $\Delta(e)$'s are displayed for $e_0 > e_g$. There are an infinity of other "linear" replacements that use both Δ_{eff} (< 1) and e^* parameters while preserving the area under the $\Delta(e)$ curve. We did not investigate this alternative since there did not appear to be any obvious way of removing the degree of freedom available in the choice of Δ_{eff} and e^* in this approach. Further, it does not produce Eq. 70 for large times.

In Figures 11, 12, and 13 we compare the predictions of the three alternative choices to the full nonlinear calculation of the maximum throughput $Q_{\max}$. We see that only Choice 3 appears to give an accurate approximation to $Q_{\max}$ over the range of ΔP, f, and ϕ_0 used. In view of the inadequacy of the approximations for Choices 1 and 2, we have not bothered to display here the analytical results that may be obtained from these approximations.

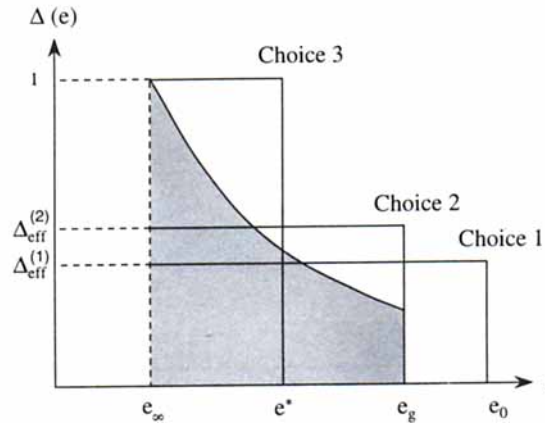

Figure 10. Three alternative choices of $\Delta(e)$ that produce to $e_0 > e_g$.

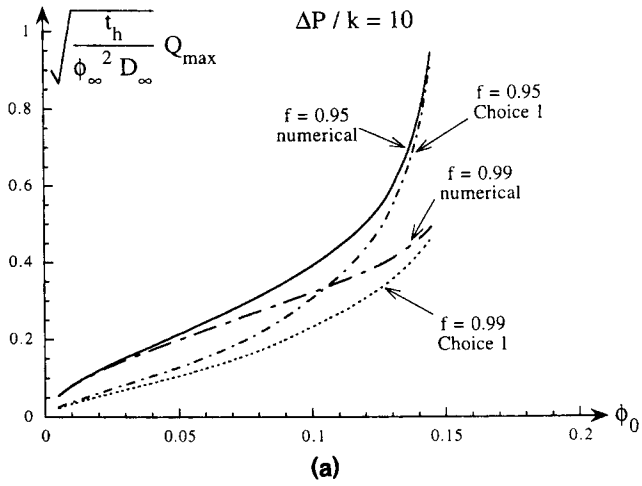

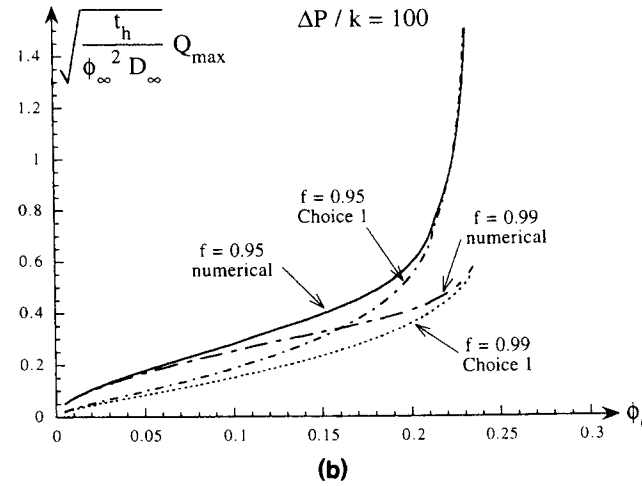

Figure 11. Comparison of the full numerical solution with the approximate linear solution using Eq. 76 (Choice 1): (a) $\Delta P/k = 10$; (b) $\Delta P/k = 100$.

Accurate Linear Approximation

In Choice 3, we solve

$$\frac{\partial e}{\partial T} = \frac{\partial}{\partial w}\left[\theta(e^* - e)\frac{\partial e}{\partial w}\right] \tag{81}$$

subject to

$$e(0,T) = e_\infty \tag{82}$$

$$\frac{\partial e}{\partial w}(1,T) = 0 \tag{83}$$

$$e(w,0) = e_0, \tag{84}$$

where e^* is given by Eq. 80. Since $e^* < e_0$ for all e_0, we always have a compact-bed formation zone in this approximation.

A similarity solution for $0 < T \le T_c$ of the form

$$e(w,T) = \begin{cases} E^*\left(\dfrac{w}{w_c(T)}\right) & (w \le w_c) \\ e_0 & (w_c < w < 1) \end{cases} \tag{85}$$

exists, with

$$w_c(T) = \left(\frac{T}{T_c}\right)^{1/2}, \tag{86}$$

where $E^*(x)$ satisfies

$$\frac{d^2E^*}{dx^2} + \frac{1}{2T_c}X\frac{dE^*}{dX} = 0, \tag{87}$$

with

$$E^*(0) = e_\infty \tag{88}$$

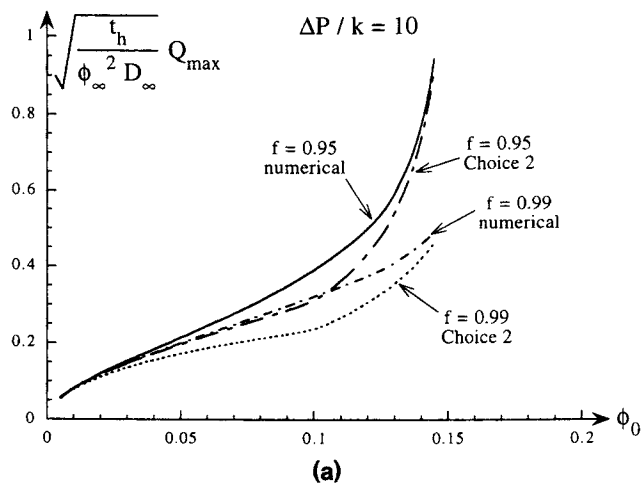

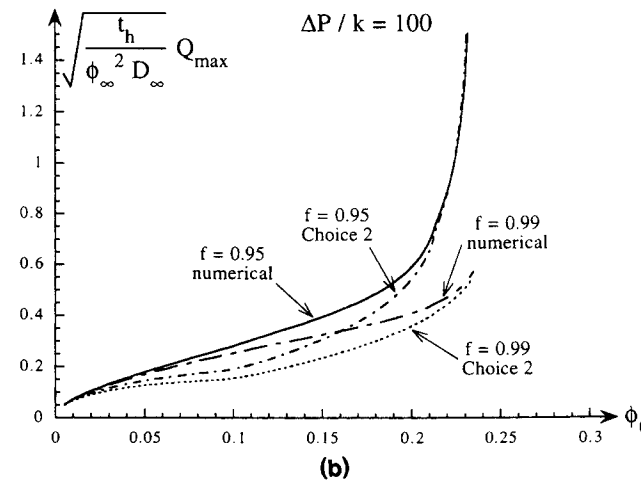

Figure 12. Comparison of the full numerical solution with the approximate linear solution using Eq. 77 (Choice 2): (a) $\Delta P/k = 10$; (b) $\Delta P/k = 100$.

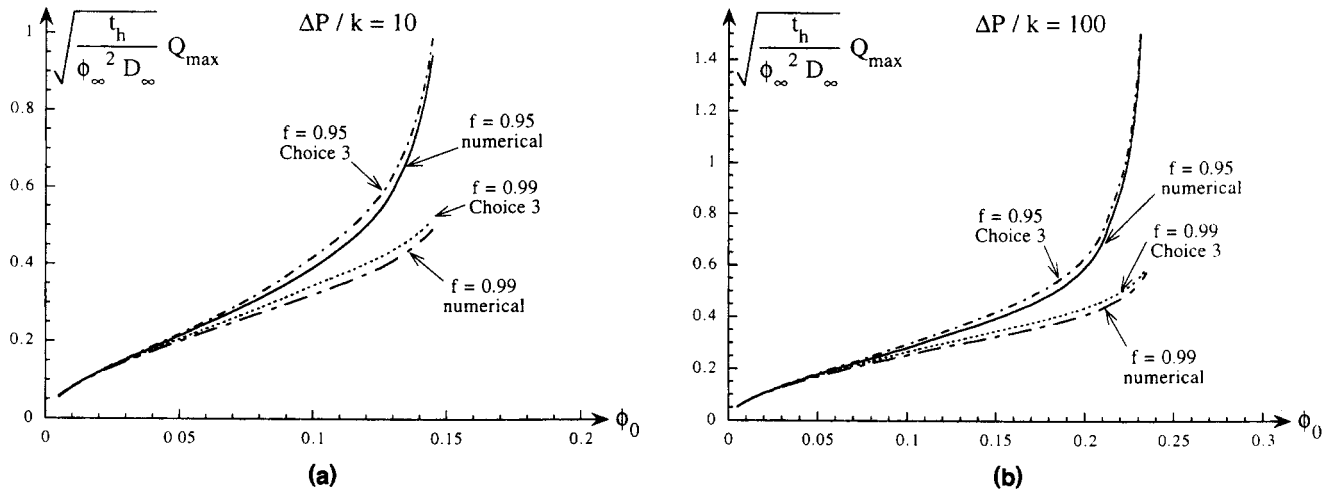

Figure 13. Comparison of the full numerical solution with the approximate linear solution using Eq. 79 (Choice 3): (a) $\Delta P/k=10$; (b) $\Delta P/k=100$.

$$E^*(1) = e^* \tag{89}$$

$$\frac{dE^*}{dX}(1) = \frac{e_0 - e^*}{2T_c}. \tag{90}$$

Here the third boundary condition allows us to solve for the unknown T_c.

The similarity solution is

$$E^*(X) = e_\infty + \frac{e_0 - e^*}{2T_c}\int_0^X dx e^{(1-x^2)/4T_c}, \tag{91}$$

where

$$\frac{e^* - e_\infty}{e_0 - e^*} = \sqrt{\pi}\,\alpha e^{\alpha^2}\mathrm{erf}(\alpha) \tag{92}$$

and

$$\alpha = \frac{1}{2T_c^{1/2}}. \tag{93}$$

In the compression region $T_c < T < \infty$ we solve

$$\frac{\partial e}{\partial T} = \frac{\partial^2 e}{\partial w^2} \quad (0 < w < 1) \tag{94}$$

subject to boundary conditions, Eqs. 57 and 58. The initial condition is

$$e(w, T_c) = E^*(w). \tag{95}$$

The solution of this problem is

$$e(w,T) = e_\infty + \sum_{n=0}^{\infty} A_n \sin[(n+1/2)\pi w] e^{-(n+1/2)^2\pi^2(T-T_c)} \tag{96}$$

where

$$A_n = 2\int_0^1 dw[E^*(w) - e_\infty]\sin[(n+1/2)\pi w]. \tag{97}$$

Substituting Eq. 91 for $E^*(w)$ and interchanging orders of integration, we obtain

$$A_n = (e^* - e_\infty)F_n, \tag{98}$$

where

$$F_n = \frac{4}{\pi^{3/2}(n+1/2)\mathrm{erf}(\alpha)}\int_0^\alpha dz e^{-z^2}\cos\left[(n+1/2)\frac{\pi z}{\alpha}\right]. \tag{99}$$

Note that F_n is a function only of the material property

$$\beta = \frac{e^* - e_\infty}{e_0 - e^*} = \frac{\int_{e_\infty}^{e_0} de\Delta(e)}{e_0 - e_\infty - \int_{e_\infty}^{e_0} de\Delta(e)} \tag{100}$$

through Eq. 92. In Figure 14, we plot the first few F_n as functions of β.

When the filtration time T_f is greater than the bed formation time T_c (certainly the case as $f \to 1$), we can use Eq. 96 to determine T_f. From Eq. 55 we have that

$$H(T) = H_\infty + \phi_0 \sum_{n=0}^{\infty} \frac{A_n}{(n+1/2)\pi} e^{-(n+1/2)^2\pi^2(T-T_c)}, \tag{101}$$

so that

$$H(T_f) = \frac{1}{f}H_\infty = H_\infty + \phi_0 \sum_{n=0}^{\infty} \frac{A_n}{(n+1/2)\pi} e^{-(n+1/2)^2\pi^2(T_f-T_c)}. \tag{102}$$

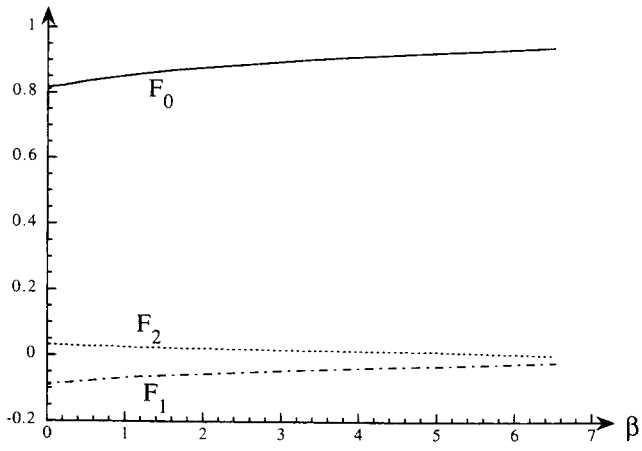

Figure 14. Fourier coefficients F_n ($n=0$, 1, 2) as functions of the material property β defined in Eq. 100.

Provided

$$T_f - T_c \gg \frac{4}{9\pi^2}, \tag{103}$$

we can abbreviate Eq. 102 to

$$\left(\frac{1}{f}-1\right)H_\infty \simeq \frac{2\phi_0 A_0}{\pi} e^{-\pi^2(T_f-T_c)/4} + \ldots. \tag{104}$$

Thus we can write

$$T_f = T_c + \frac{4}{\pi^2}\ln\left\{\frac{2\phi_\infty A_0 f}{\pi(1-f)}\right\} + \ldots. \tag{105}$$

It is possible that the stopping fraction f or initial volume fraction ϕ_0 is such that T_f occurs during the compact-bed formation stage. In this case (see Appendix B)

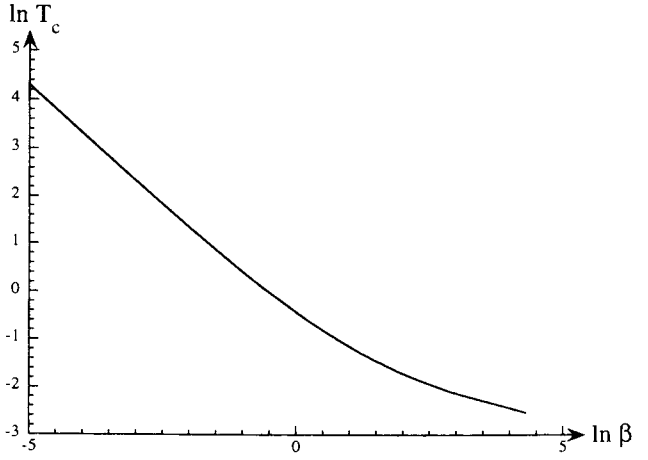

Figure 15. Scaled-bed-formation time ln T_c as a function of ln β defined in Eq. 100.

$$T_f = T_c e^{-1/(2T_c)}\left[\frac{1+e_0-\frac{1}{f}(1+e_\infty)}{e_0-e^*}\right]^2. \tag{106}$$

In Figure 15 we display T_c as a function of β as calculated from Eqs. 92 and 93. For small β the asymptotic result (Hill and Dewynne, 1987)

$$T_c = \frac{1}{2}\left[\frac{1}{\beta}+\frac{1}{3}-\frac{2\beta}{45}+\frac{16\beta^2}{945}+\cdots\right] \tag{107}$$

may be used with the two-term approximation

$$T_c \approx \frac{1}{2}\left[\frac{1}{\beta}+\frac{1}{3}\right], \tag{108}$$

accurate to a few percent for $0<\beta\lesssim 2$. For large β, we can use the asymptotic result

$$T_c = \left[4\ln\left(\frac{\beta+1}{\sqrt{\pi}}\right)-2\ln\ln\left(\frac{\beta+1}{\sqrt{\pi}}\right)+O\left(\frac{1}{\beta\ln\beta}\right)\right]^{-1}, \tag{109}$$

accurate to a few percent for $\beta \gtrsim 4$. For the region between these asymptotic results, T_c may be read from Figure 15 or calculated from Eq. 92.

Conclusions and Implications to Pressure-Filter Design

The analysis of the maximized throughput together with the linear approximate method allows us to make some strong conclusions about pressure-filter design. We know how the maximized throughput depends on the filtration time and have been able to obtain simple accurate estimates of the filtration time in terms of the rheological parameters that define the mechanics of the suspension.

In the first place, the rheological functions $P_y(\phi)$ and $D(\phi)$ for the suspension must be measured, the ϕ_∞ obtained from the chosen applied pressure (Eq. 4), and the desired stopping fraction f chosen.

The key question in pressure-filter design asks what filter area is required to process a volumetric throughput q in the plant, from an initial solids fraction ϕ_0 to a final average volume fraction $f\phi_\infty$.

The results show that to optimally process solids to average volume fraction $f\phi_\infty$ at a rate q, we must load our filter press so that the filtration time is equal to handling time for the press, as discussed earlier.

The filter surface area required is calculated by

$$A = \frac{q}{Q_{\max}} \tag{110}$$

$$= \frac{2qT_f^{1/2}t_h^{1/2}}{\phi_\infty D_\infty^{1/2}}. \tag{111}$$

The optimal loading is

$$h_0^{\max} = \left(\frac{\phi_\infty}{\phi_0}\right)\frac{D_\infty^{1/2} t_h^{1/2}}{T_f^{1/2}}, \tag{112}$$

and this clearly shows its dependence on the scaled filtration time T_f.

In order to calculate this quantity, both e^* and β must be calculated for ϕ_0 and ϕ_∞, from $D(\phi)$ data from Eqs. 80 and 100. Then T_f is given by

$$T_f = \left\{T_c + \frac{4}{\pi^2}\ln\frac{2F_0}{\pi}\right\} + \frac{4}{\pi^2}\ln\left[\frac{f\phi_\infty(e^* - e_\infty)}{1-f}\right], \tag{113}$$

where the $T_c(\beta)$ and $F_0(\beta)$ may be computed by Eqs. 92, 93 and 99 or, with reasonable accuracy, simply taken off Figures 14 and 15.

This value can be substituted back into Eq. 111 to obtain the required filter surface area, and optimal loading (Eq. 112).

If we regard ϕ_0 and $f\phi_\infty$ as fixed, we can still exert a degree of freedom through the choice of ϕ_∞, which is controlled by the applied pressure ΔP. By increasing ΔP and decreasing the stopping fraction f (to keep $f\phi_\infty$ constant), we cause $Q_{\max}$ to increase, as shown in Figures 13a, 13b.

The design of a pressure-filter operation is, by this procedure, reduced to a knowledge of the quantity e^* as a function of ϕ_0 and ϕ_∞. This in turn requires a knowledge of $\Delta(e)$ $[D(\phi)]$ over the range of void ratios spanned. It is therefore important to devise straightforward methods of estimating $D(\phi)$ from experimental filtration data on the bench in order to usefully scale up the operation to the plant. We will address this matter in a subsequent article.

Acknowledgment

The authors thank the Australian Research Council and the International Fine Particle Research Institute for financial support.

Literature Cited

Auzerais, F. M., R. Jackson, W. B. Russel, and W. F. Murphy, "The Transient Settling of Stable and Flocculated Dispersions," *J. Fluid Mech.*, **221**, 613 (1990).

Banks, P. J., "Theory of Constant-Rate Expression and Subsequent Relaxation," *Drying*, R. Toei and A. S. Mujumdar, eds., Hemisphere, New York, p. 102 (1985).

Buscall, R., and L. R. White, "On the Consolidation of Concentrated Suspensions I: The Theory of Sedimentation," *J. Chem. Soc. Farad. Trans.*, **83** (1), 873 (1987).

Channell, G. M., and C. F. Zukoski, "Shear and Compressive Rheology of Aggregated Alumina Suspensions," *AIChE J.*, **43**, 1700 (1997).

Eberl, M., K. A. Landman, and P. J. Scales, "Scale-Up Procedures and Test Methods in Filtration: A Test Case on Kaolin Plant Data," *Colloids Sci. A*, **103**, 1 (1995).

Eckert, W. F., J. H. Masliyah, M. R. Gray, and P. M. Fedorak, "Prediction of Sedimentation and Consolidation of Fine Tails," *AIChE J.*, **42**, 960 (1996).

Green, M. D., *Characterization of Suspensions in Settling and Compression*, PhD Thesis, Univ. of Melbourne, Melbourne, Australia (1997).

Hill, J. M., and J. N. Dewynne, *Heat Conduction*, Blackwell, Oxford (1987).

Kirby, J. M., and D. E. Smiles, "Hydraulic Conductivity of Aqueous Bentonite Suspensions," *Aust. J. Soil Res.*, **26**, 561 (1988).

Landman, K. A., C. Sirakoff, and L. R. White, "Dewatering of Flocculated Suspensions by Pressure Filtration," *Phys. Fluids A*, **3**, 1495 (1991).

Landman, K. A., and L. R. White, "Solid-Liquid Separation of Flocculated Suspensions," *Adv. Colloid Interface Sci.*, **51**, 175 (1994).

Landman, K. A., L. R. White, and M. Eberl, "Pressure Filtration of Flocculated Suspensions," *AIChE J.*, **41**, 1687 (1995).

McNabb, A., "Asymptotic Behaviour of Solutions of a Stephan Problem," *J. Math. Anal. Appl.*, **51**, 633 (1975).

Miller, K. T., R. M. Melant, and C. F. Zukoski, "Comparison of the Compression Response of Aggregated Suspensions: Pressure Filtration, Centrifugation, and Osmotic Consolidation," *J. Amer. Ceram. Soc.*, **79**, 2545 (1996).

Phillip, J. R., and D. E. Smiles, "Macroscopic Analysis of the Behavior of Colloidal Suspensions," *Adv. Colloid Interf. Sci.*, **17**, 83 (1982).

Shirato, M., T. Murase, and N. Hayashi, "Expression Theory and Its Practical Utilization," *Proc. World Filtration Cong. III*, vol. 1, Filtration Society, Croydon, England, p. 280 (1982).

Sivaram, B., and P. K. Swamee, "A Computational Method for Consolidation Coefficient," *J. Jpn. Soc. Soil Mech. Found. Eng.*, **17**, 48 (1977).

Smiles, D. E., and J. M. Kirby, "Aspects of One-Dimensional Filtration," *Sep. Sci. Technol.*, **22**, 1405 (1987).

Terzaghi, K., and P. B. Peck, *Soil Mechanics in Engineering Practice*, Wiley, New York (1948).

Appendix A: Properties of $T^*(w)$

We note that, as should be expected,

$$T^*(0) = 0 \tag{A1}$$

by virtue of Eq. 57. In addition, we see that

$$\frac{d^2T^*}{dw^2}(w) = \frac{\int_0^\infty dT \frac{\partial^2}{\partial w^2}\int_{e_\infty}^{e(w,T)} de\Delta(e)}{\int_{e_\infty}^{e_0} de\Delta(e)} \tag{A2}$$

$$= \frac{\int_0^\infty dT \frac{\partial}{\partial w}\left[\Delta(e)\frac{\partial e}{\partial w}\right]}{\int_{e_\infty}^{e_0} de\Delta(e)} \tag{A3}$$

$$= \int_0^\infty dT \frac{\partial e}{\partial T} \Big/ \int_{e_\infty}^{e_0} de\Delta(e) \tag{A4}$$

$$= -(e_0 - e_\infty)/\int_{e_\infty}^{e_0} de\Delta(e). \tag{A5}$$

To completely determine $T^*(w)$, we need another boundary condition. We note that

$$\frac{dT^*}{dw}(0) = \int_0^\infty dT \frac{\partial e}{\partial w}(0,T)/\int_{e_\infty}^{e_0} de\Delta(e) \tag{A6}$$

with the aid of Eq. 61. From Eq. 55 we have that

$$\frac{dH}{dT} = \phi_0\int_0^1 dw \frac{\partial e}{\partial T}(w,T) \tag{A7}$$

$$= \phi_0\int_0^1 dw \frac{\partial}{\partial w}\left[\Delta(e)\frac{\partial e}{\partial w}\right] \tag{A8}$$

$$= -\phi_0 \frac{\partial e}{\partial w}(0,T) \tag{A9}$$

after integration and use of Eq. 58. We can therefore write

$$\frac{dT^*}{dw}(0) = -\frac{1}{\phi_0}\int_0^\infty dT \frac{dH}{dT} \Big/ \int_{e_\infty}^{e_0} de\Delta(e) \tag{A10}$$

$$= (e_0 - e_\infty) / \int_{e_\infty}^{e_0} de\Delta(e) \tag{A11}$$

with the aid of Eqs. 24, 57 and 59.

Appendix B: T_f for $T_f < T_c$

If $T_f < T_c$, then, clearly,

$$H(T_c) < H(T_f) = \frac{1}{f} H_\infty. \tag{B1}$$

From Eq. 55 we have that

$$H(T_c) = \phi_0 \left[1 + \int_0^1 dX E^*(X)\right], \tag{B2}$$

so that $T_f < T_c$, provided

$$\frac{1}{f\phi_\infty} - 1 > \int_0^1 dX E^*(X). \tag{B3}$$

The similar solution Eq. 91 is used to show that

$$\int_0^1 dX E^*(X) = e_0 - (e_0 - e^*)e^{\alpha^2}. \tag{B4}$$

Thus $T_f < T_c$, provided

$$\frac{1}{f\phi_\infty} - 1 > e_0 - (e_0 - e^*)e^{\alpha^2}. \tag{B5}$$

In this regime, we find T_f as follows. In the similarity regime, we have that

$$H(T) = 1 - [1 - H(T_c)]\left(\frac{T}{T_c}\right)^{1/2} \tag{B6}$$

from Eq. 55. Thus

$$H(T_f) = \frac{1}{f} H_\infty = 1 - [1 - H(T_c)]\left(\frac{T_f}{T_c}\right)^{1/2} \tag{B7}$$

and

$$T_f = T_c \left[\frac{1 - \frac{1}{f}H_\infty}{1 - H(T_c)}\right]^2 \tag{B8}$$

$$= T_c \left[\frac{1 + e_0 - \frac{1}{f}(1 + e_\infty)}{e_0 - e^*}\right]^2 e^{-2\alpha^2}. \tag{B9}$$

Manuscript received Apr. 28, 1997, and revision received Aug. 11, 1997.